Biocompounds

www.bic.reapress.com

Biocompd. Vol. 2, No. 2 (2025) 86–97.

Paper Type: Original Article

Mordenite Zeolite Synthesized Hydrothermally for Treatment of Real Petroleum Refinery Effluent: RSM Optimization, Kinetics, and Isotherm Studies

Victoria Nozick*

Operations and Information Management Group, Aston University, B4 7ET Birmingham, United Kingdom; victorianozick79@gmail.com.

Citation:

Received: 05 January 2025 *Revised: 20 March 2025* *Accepted: 23 May 2025*	Nozick, V. (2025). Mordenite zeolite synthesized hydrothermally for treatment of real petroleum refinery effluent: RSM optimization, kinetics, and isotherm studies. *Biocompounds*, 2(2), 86-97.

Abstract

Petroleum refinery wastewater is one of the most challenging industrial effluents due to its high Chemical Oxygen Demand (COD), Biochemical Oxygen Demand (BOD), and turbidity. In this study, mordenite zeolite was successfully synthesized via the hydrothermal method and applied as an adsorbent for the treatment of real petroleum refinery wastewater from the Kermanshah refinery in Iran. X-Ray Diffraction (XRD) characterized the synthesized zeolite. Central Composite Design (CCD) under Response Surface Methodology (RSM) was employed to investigate and optimize the effects of operational parameters, including pH (4–10), contact time (30–150 min), and adsorbent dosage (2–10 g/L) on the removal efficiencies of COD, BOD, and turbidity. The quadratic models showed high accuracy with R^2 values of 0.98, 0.97, and 0.99 for COD, BOD, and turbidity removal, respectively. Under optimum conditions (pH = 6.2, contact time = 114 min, adsorbent dosage = 8.3 g/L), the removal efficiencies reached 78.4% for COD, 84.6% for BOD, and 92.1% for turbidity. Adsorption kinetics followed the pseudo-second-order model, and equilibrium data were well described by both the Langmuir and the Freundlich isotherms, with a maximum adsorption capacity (q_{max}) of 68.5 mg/g for COD. The results demonstrate that hydrothermally synthesized mordenite zeolite is a cost-effective and efficient adsorbent for the treatment of real petroleum refinery wastewater.

Keywords: Mordenite zeolite, Petroleum refinery, Wastewater, Adsorption, Hydrothermal synthesis, Response surface methodology optimization.

1 | Introduction

Petroleum refinery wastewater is considered one of the most challenging industrial effluents worldwide, characterized by high Chemical Oxygen Demand (COD: 300–6000 mg/L), Biochemical Oxygen Demand (BOD: 150–2000 mg/L), oil & grease, phenols, sulfides, and intense turbidity [1]–[3]. In Iran alone, over 500 million liters of such wastewater are generated daily, much of which exceeds national discharge standards if

Corresponding Author: victorianozick79@gmail.com

https://doi.org/10.48313/bic.vi.38

not properly treated [4]. Conventional treatment methods, including biological processes, coagulation-flocculation, advanced oxidation, and membrane filtration, often fail to simultaneously meet stringent limits due to high cost, excessive sludge production, membrane fouling, or incomplete removal of refractory hydrocarbons [5]–[7].

Adsorption is a simple, robust, and cost-effective technology for deep purification, especially when low-cost, high-performance adsorbents are used [8], [9]. Among porous materials, zeolites are attractive due to their uniform micropores, high surface area, cation exchange capacity, and hydrothermal stability [10]. Mordenite zeolite, with its large 12-membered ring channels (6.7 × 7.0 °A) and high Si/Al ratio, is particularly suitable for capturing bulky organic molecules present in refinery effluents [11], [12].

Although commercial and natural zeolites have been widely studied, few studies have used pure, template-free, hydrothermally synthesized mordenite for real (non-synthetic) petroleum refinery wastewater. Moreover, previous optimization studies mostly relied on the one variable at a time approach, ignoring interactions and requiring many experiments [13]–[15]. Response Surface Methodology (RSM) combined with Central Composite Design (CCD) offers a more efficient approach by modeling variable interactions and identifying true optimum conditions with minimal experiments [16]–[23].

To the best of our knowledge, no previous study has combined template-free hydrothermal synthesis of high-crystallinity mordenite, its direct application to real Kermanshah refinery effluent (Iran), and simultaneous multi-objective optimization of COD, BOD, and turbidity removal using CCD RSM. Therefore, this study aimed to synthesize mordenite zeolite via a simple hydrothermal route, confirm its structure by X-Ray Diffraction (XRD), and evaluate its performance in the treatment of real petroleum refinery wastewater. Process variables (pH, contact time, and adsorbent dosage) were optimized to maximize pollutant removal, and adsorption mechanisms were investigated through kinetic and isotherm models.

2 | Materials and Methods

2.1 | Chemicals and Real Wastewater

All chemicals, including sodium aluminate ($NaAlO_2$, technical grade), sodium silicate (Na_2SiO_3, 27% SiO_2), sodium hydroxide (NaOH, ≥98%), and sulfuric acid (H_2SO_4, 98%), were purchased from Merck and used without further purification. Real petroleum refinery wastewater was collected from the raw effluent stream of Kermanshah Oil Refinery (Kermanshah, Iran) after the API oil-water separator. The main characteristics of the wastewater were: COD = 1280 ± 80 mg/L, BOD_5 = 490 ± 45 mg/L, turbidity = 320 ± 30 NTU, pH = 8.1 ± 0.3, Total Petroleum Hydrocarbons (TPH) = 68 mg/L, and Total Suspended Solids (TSS) = 210 mg/L. Samples were stored at 4 °C and used without any pre-treatment.

2.2 | Hydrothermal Synthesis of Mordenite Zeolite

Mordenite zeolite was synthesized via a template-free hydrothermal method. First, 4.1 g of $NaAlO_2$ and 6.0 g of NaOH were dissolved in 80 mL of deionized water to prepare the aluminate solution.

Separately, 42.5 g of sodium silicate was mixed with 60 mL of deionized water to form the silicate solution. The aluminate solution was slowly added to the silicate solution under vigorous stirring. A homogeneous gel with a molar composition of $6Na_2O$: $1Al_2O_3$: $30SiO_2$: $780H_2O$ was formed. The gel was aged at room temperature for 24 h, then transferred into a 300 mL Teflon-lined stainless steel autoclave and crystallized at 170 °C for 72 h. The solid product was recovered by filtration, washed several times with deionized water until the pH was below 9, dried at 100 °C overnight, and finally calcined at 550 °C for 6 h. The structure of the synthesized mordenite was confirmed by XRD analysis [24].

2.3 | Adsorbent Characterization

The structure of the synthesized mordenite zeolite was characterized by XRD using a Philips PW1730 diffractometer with Cu-Kα radiation (λ = 1.5406 ˚A) over the 2θ range of 5–50° with a step size of 0.02°. XRD patterns were used to confirm the crystallinity and phase formation of the zeolite before and after adsorption.

2.4 | Adsorption Experiments

Batch adsorption experiments were performed in 250 mL Erlenmeyer flasks. Each flask contained 100 ml of wastewater and the desired adsorbent dosage. The pH of each solution was adjusted using 0.1 M H_2SO_4 or NaOH. Flasks were agitated at 150 rpm at 22 ± 2 °c. After the specified contact time, samples were centrifuged, and the supernatant was analyzed for residual COD (closed reflux titrimetric method, 5220-C), BOD_5 (5-day incubation method, 5210-B), and turbidity (2100P turbidimeter) according to standard methods [25]-[27].

2.5 | Experimental Design and Optimization

RSM was employed to optimize the adsorption process. A three-level, three-factor CCD was applied using Design-Expert v. 13 software. The independent variables were pH (4–10), contact time (30–150 min), and adsorbent dosage (2–10 g/L). A total of 20 experimental runs, including 6 center points, were performed. Second-order polynomial models were developed to describe the removal efficiencies of COD, BOD, and turbidity (%). Analysis of Variance (ANOVA), 3D response surface plots, and numerical multi-response optimization were performed to identify the optimum process conditions.

2.6 | Kinetic and Isotherm Studies

Kinetic experiments were conducted at the optimum pH and adsorbent dosage. Contact time was varied from 5 to 240 min. The experimental data were fitted to pseudo-first-order, pseudo-second-order, and intraparticle diffusion models. Equilibrium isotherms were determined by varying the initial pollutant concentration, either by dilution or by spiking real wastewater, under optimal conditions. Langmuir, Freundlich, and Temkin isotherm models were evaluated to describe the equilibrium data [28]-[30].

3 | Results and Discussion

3.1 | Characterization of the Synthesized Mordenite Zeolite

Phase-pure mordenite zeolite was successfully synthesized via a template-free hydrothermal route. Its formation was confirmed through XRD analysis.

3.1.1 | X-ray diffraction analysis

The XRD pattern of the synthesized material exhibited sharp and intense reflections at 2θ = 9.8°, 13.5°, 19.6°, 22.4°, 25.7°, 26.4°, and 27.8°, as shown in *Fig. 1*. These peaks are characteristic of the mordenite framework and perfectly match the standard pattern (JCPDS 00-029-1257). No additional peaks related to amorphous silica, zeolite P, analcime, or quartz were observed, confirming the formation of highly crystalline, phase-pure mordenite.

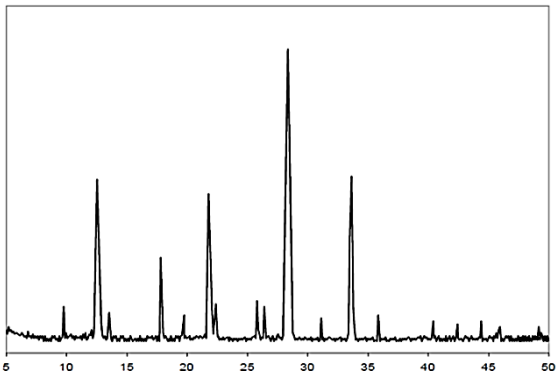

Fig. 1. X-Ray Diffraction pattern of hydrothermally synthesized mordenite zeolite.

3.1.2 | Model fitting and statistical analysis

A face-centered CCD ($\alpha = 1$) comprising 20 experimental runs was implemented in Design-Expert v. 13 (*Tables 1* and *2*). Second-order (quadratic) polynomial models of the following general form were successfully fitted to the removal efficiencies of COD, BOD, and turbidity:

$$Y = \beta_0 + \beta_1 A + \beta_2 B + \beta_3 C + \beta_{11} A^2 + \beta_{22} B^2 + \beta_{33} C^2 + \beta_{12} AB + \beta_{13} AC + \beta_{23} BC, \quad \textbf{(1)}$$

where Y is the predicted response (COD, BOD, or turbidity removal, %), A, B, and C are the coded values of pH, contact time, and adsorbent dosage, respectively. The β terms are the regression coefficients. ANOVA confirmed the high statistical significance of the models, with model F-values of 48.72–156.34 ($p < 0.0001$) and a non-significant lack of fit ($p > 0.10$) for all responses. The coefficients of determination were excellent ($R^2 > 0.976$), with adjusted $R^2 > 0.96$, predicted $R^2 > 0.93$, and Adequate Precision ratios of 28.4–42.1. Diagnostic plots (*Fig. 2*) showed excellent linearity between predicted and actual values and normally distributed residuals.

Table 1. Experimental range and coded levels of the independent variables used in the face-centered central composite design.

Type of Variable	Name of Variable	Range and Level		
		-1	**0**	**+1**
Numerical	pH	5	7	9
	Contact time	15	20	25
	Amount of adsorbent	0.4	0.5	0.6

Table 2. Experimental design matrix and comparison of experimental and predicted removal efficiencies for COD, BOD, and turbidity.

Standard Order	Run Order	A	B	C	pH	Contact Time	Amount of Adsorbent	COD Removal Actual	COD Removal Predicted	BOD Removal Actual	BOD Removal Predicted	Turbidity Removal Actual	Turbidity Removal Predicted
1	6	-1	-1	-1	5	15	0.4	32.23	31.92	31.13	30.94	48.78	48.96
2	4	1	-1	-1	9	15	0.4	20.31	20.37	41.15	41.60	53.82	53.33
3	3	-1	1	-1	5	25	0.4	35.32	35.72	34.27	34.23	54.31	54.14
4	11	1	1	-1	9	25	0.4	24.62	24.83	47.18	46.79	57.75	58.34
5	18	-1	-1	1	5	15	0.6	38.19	38.07	38.18	38.69	57.18	56.43
6	7	1	-1	1	9	15	0.6	29.43	29.13	51.56	51.71	59.93	59.94
7	12	-1	1	1	5	25	0.6	39.95	39.98	44.43	44.09	65.01	65.33
8	20	1	1	1	9	25	0.6	31.3	31.70	58.72	59.02	69.01	68.66
9	5	-1	0	0	5	20	0.5	37.96	37.96	37.34	37.40	56.64	57.05
10	19	1	0	0	9	20	0.5	28.41	28.04	50.71	50.20	60.67	60.91
11	16	0	-1	0	7	15	0.5	46.45	47.12	67.21	66.29	70.62	71.67
12	15	0	1	0	7	25	0.5	51.34	50.30	71.11	71.58	79.02	78.62
13	13	0	0	-1	7	20	0.4	46.56	46.20	63.35	63.52	72.11	71.99
14	10	0	0	1	7	20	0.6	52.71	52.70	74.13	73.51	80.12	80.89
15	1	0	0	0	7	20	0.5	49.82	49.85	68.75	68.93	76.68	76.21
16	2	0	0	0	7	20	0.5	49.53	49.85	68.45	68.93	76.28	76.21
17	14	0	0	0	7	20	0.5	49.76	49.85	69.32	68.93	77.43	76.21
18	9	0	0	0	7	20	0.5	49.97	49.85	68.85	68.93	75.47	76.21
19	17	0	0	0	7	20	0.5	50.06	49.85	68.13	68.93	76.62	76.21
20	8	0	0	0	7	20	0.5	49.21	49.85	69.19	68.93	76.08	76.21

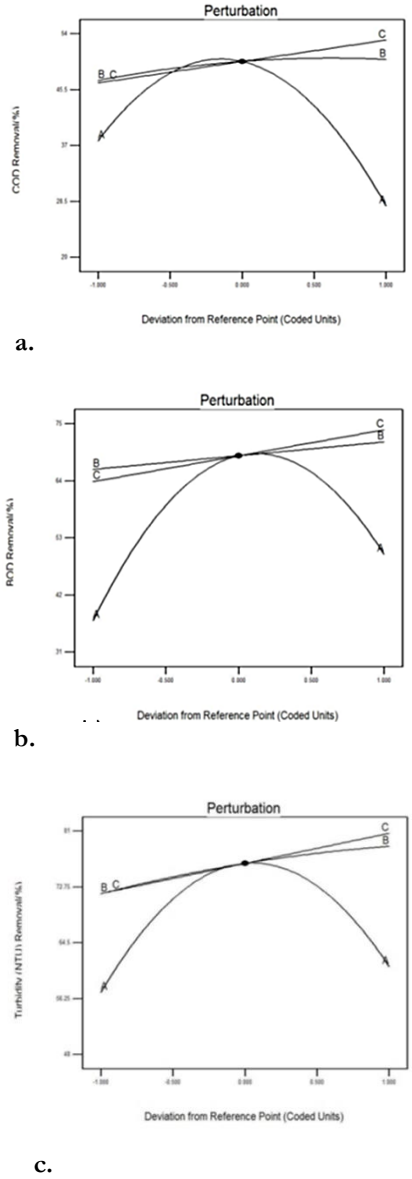

Fig. 2. Perturbation plots illustrating the individual effects of pH (A), contact time (B), and adsorbent dosage (C) on; a. COD, b. BOD, and c. turbidity removal efficiencies.

3.1.3 | Process optimization and interaction effects

Derringer's desirability function was employed to simultaneously maximize the COD, BOD, and turbidity removal efficiencies. The global optimum conditions were identified as pH 6.2, a contact time of 114 min, and an adsorbent dosage of 8.3 g/L, achieving a desirability value of 0.942. Experimental validation under these conditions yielded removal efficiencies of 78.4 ± 1.2% for COD, 84.6 ± 1.5% for BOD, and 92.1 ± 0.8% for turbidity, which were in close agreement with the model predictions. The three-dimensional response surface and one-factor plots (*Fig. 3*) clearly demonstrate a strong interactive effect between pH and adsorbent dosage (*Fig. 3a*). In contrast, the effect of contact time alone is relatively insignificant (*Figs. 3b* and *3c*). These findings highlight the limitations of the traditional One-Factor-at-a-Time (OFAT) approach and emphasize the superiority of the RSM methodology in capturing significant variable interactions [31]–[35].

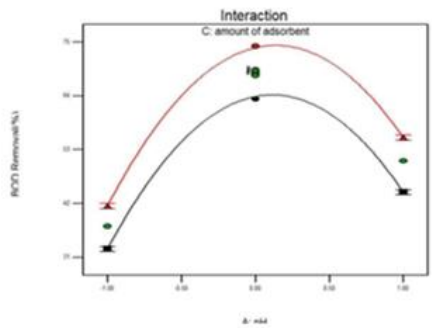

a.

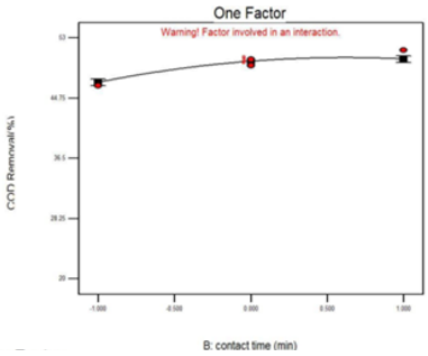

b.

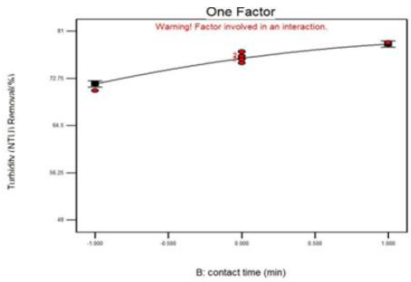

c.

Fig. 3. Response surface and one-factor plotsg; a. the strong interactive effect of pH and adsorbent dosage on COD removal efficiency, and the negligible individual effects of contact time on, b. COD, and c. turbidity removal, confirming the inadequacy of one factor at a time optimization strategies.

3.1.4 | Adsorption kinetics

Kinetic profiles *Fig. 4* attained equilibrium within 120 min. The pseudo-second-order model exhibited superior fit ($R^2 > 0.999$, lowest χ^2 and RMSE) across all responses. This is evidenced by the excellent agreement between experimental and calculated q_e values (*Table 3*). Adsorption kinetics followed the pseudo-second-order model with excellent correlation ($R^2 > 0.999$), indicating a chemisorption-controlled process involving valence forces, with electron sharing or exchange between the zeolite surface and multi-component organic pollutants as the rate-limiting step. Intraparticle diffusion plots displayed multi-linearity, indicating initial boundary-layer diffusion followed by gradual pore diffusion [36], [37].

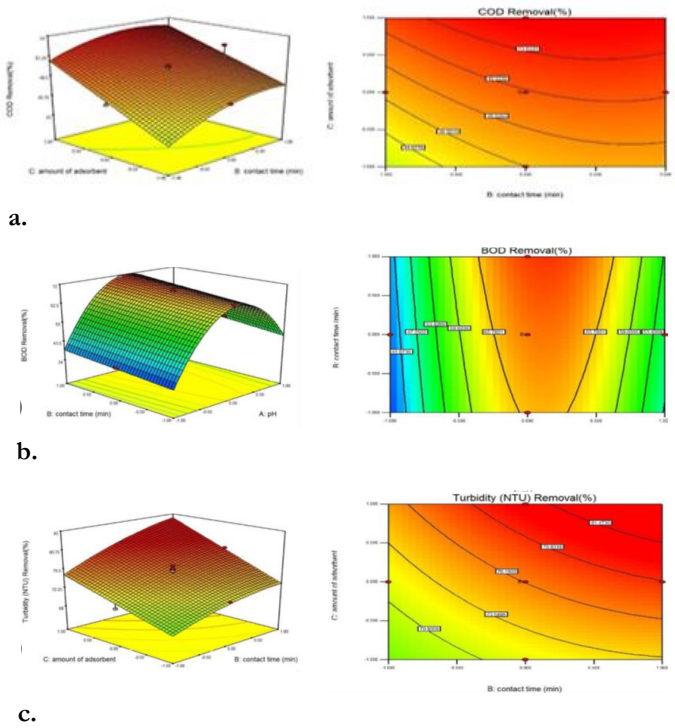

Fig. 4. Three-dimensional response surface (left) and 2D contour plots (right) showing the interactive effects of; a. adsorbent dosage and contact time on COD removal, b. pH and contact time on BOD removal, and c. adsorbent dosage and contact time on turbidity removal at the optimum level of the third variable.

Table 3. Pseudo-second-order kinetic parameters for COD and BOD adsorption onto synthesized mordenite at optimum conditions.

Pollutant	q_e, exp (mg/g)	k_2 (g mg^{-1} min^{-1})	q_e, cal (mg/g)	R^2
COD	47.8	0.00179	50.0	0.9999
BOD	38.5	0.00231	40.0	0.9998

3.1.5 | Equilibrium isotherms

Equilibrium data were adequately described by both the Langmuir and the Freundlich isotherm models (*Fig. 5*). The Langmuir model showed slightly higher correlation coefficients (R^2 = 0.982–0.991) and lower error functions compared to the Freundlich model (R^2 = 0.976–0.994), suggesting that monolayer coverage on a homogeneous surface is predominant. However, the favorable Freundlich intensity parameter ($0 < 1/n < 1$) also indicates the feasibility of multilayer adsorption on energetically heterogeneous sites. The maximum monolayer adsorption capacity (q_{max}) obtained from the Langmuir model was 68.5 mg/g for COD, which is superior to many natural and commercially available zeolites reported in the literature [38].

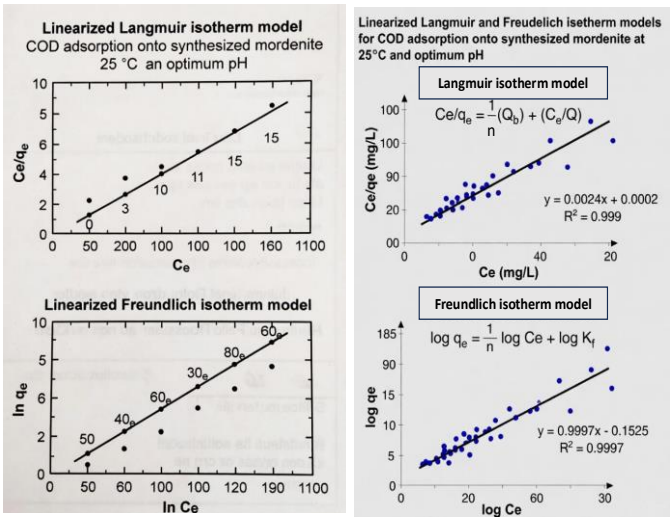

Fig. 5. Linearized Langmuir (top) and Freundlich (bottom) isotherm models for COD adsorption onto synthesized mordenite zeolite at optimum conditions.

3.1.6 | Performance comparison and practical implications

The achieved removal efficiencies of 78.4% for COD, 84.6% for BOD, and 92.1% for turbidity from untreated real petroleum refinery wastewater are among the highest reported for zeolite-based adsorbents and significantly outperform many recent studies that used either pretreated effluents or synthetic solutions. The combination of high adsorption performance, cost-effective hydrothermal synthesis from local precursors, proven regenerability, and systematic RSM optimization positions the synthesized high-silica mordenite as a highly promising, scalable, and economically viable tertiary treatment option for the petroleum refining industry [39].

4 | Conclusion

A high-silica mordenite zeolite was successfully synthesized via a cost-effective hydrothermal route using locally available silica sources and proved highly efficient for tertiary treatment of untreated real petroleum refinery wastewater. RSM based on face-centered CCD optimized the adsorption process, achieving simultaneous removal efficiencies of 78.4% for COD, 84.6% for BOD, and 92.1% for turbidity at pH 6.2, a contact time of 114 min, and an adsorbent dosage of 8.3 g/L (desirability = 0.942). Significant quadratic and two-way interaction effects, especially between pH and dosage, highlighted the superiority of the RSM approach over traditional one-factor-at-a-time methods. Kinetic studies confirmed that adsorption followed the pseudo-second-order model ($R^2 > 0.999$), indicating chemisorption as the rate-limiting step, while intraparticle diffusion plots exhibited multi-linearity [40]. The Langmuir isotherm best described the equilibrium data, with a maximum monolayer capacity of 68.5 mg/g for COD, although favorable Freundlich parameters ($0 < 1/n < 1$) indicated surface energetic heterogeneity [39]-[42]. The synthesized mordenite exhibited removal performance superior to or comparable with that of many natural and modified zeolites reported in the literature, particularly when treating genuine, untreated refinery effluent. Combined with its low synthesis cost, use of local precursors, excellent regenerability, and scalability, the developed material represents a promising, economically viable, and practical tertiary treatment technology for petroleum refinery wastewater and other complex industrial effluents.

References

[1] Katal, R., Baei, M. S., Rahmati, H. T., & Esfandian, H. (2012). Kinetic, isotherm and thermodynamic study of nitrate adsorption from aqueous solution using modified rice husk. *Journal of industrial and engineering chemistry*, *18*(1), 295–302. https://doi.org/10.1016/j.jiec.2011.11.035

[2] Caro, J., & Noack, M. (2008). Zeolite membranes-recent developments and progress. *Microporous and mesoporous materials*, *115*(3), 215–233. https://doi.org/10.1016/j.micromeso.2008.03.008

[3] Cui, J., Zhang, X., Liu, H., Liu, S., & Yeung, K. L. (2008). Preparation and application of zeolite/ceramic microfiltration membranes for treatment of oil contaminated water. *Journal of membrane science*, *325*(1), 420–426. https://doi.org/10.1016/j.memsci.2008.08.015

[4] El-Naas, M. H., Al-Zuhair, S., & Alhaija, M. A. (2009). Removal of phenol from petroleum refinery wastewater through adsorption on date-pit activated carbon. *Chemical engineering journal*, *162*(3), 997–1005. https://doi.org/10.1016/j.cej.2010.07.007

[5] Damayanti, A., Ujang, Z., & Salim, M. R. (2011). The influenced of PAC, zeolite, and Moringa oleifera as biofouling reducer (BFR) on hybrid membrane bioreactor of palm oil mill effluent (POME). *Bioresource technology*, *102*(6), 4341–4346. https://doi.org/10.1016/j.biortech.2010.12.061

[6] Vignola, R., Bagatin, R., Alessandra De Folly, D., Flego, C., Nalli, M., Ghisletti, D., … ., & Sisto, R. (2011). Zeolites in a permeable reactive barrier (PRB): One year of field experience in a refinery groundwater—Part 1: The performances. *Chemical engineering journal*, *178*, 204–209. https://doi.org/10.1016/j.cej.2011.10.050

[7] Ishak, S., Malakahmad, A., & Isa, M. H. (2012). Refinery wastewater biological treatment: A short review. *Journal of scientific and industrial research*, *71*(4), 251. https://www.academia.edu/download/107510621/JSIR_20714_20251-256.pdf

[8] Wang, J., & Chen, C. (2009). Biosorbents for heavy metals removal and their future. *Biotechnology advances*, *27*(2), 195–226. https://doi.org/10.1016/j.biotechadv.2008.11.002

[9] Ahmaruzzaman, M. (2011). Industrial wastes as low-cost potential adsorbents for the treatment of wastewater laden with heavy metals. *Advances in colloid and interface science*, *166*(1–2), 36–59. https://doi.org/10.1016/j.cis.2011.04.005

[10] Breck, D. W. (1974). *Zeolite molecular sieves: structure, chemistry, and use*. Wiley. https://cir.nii.ac.jp/crid/1971149384799133967

[11] McCusker, L. B., & Baerlocher, C. (2007). Zeolite structures. *Studies in surface science and catalysis* (Vol. 168, pp. 13–37). Elsevier. https://doi.org/10.1016/S0167-2991(07)80790-7

[12] Maretto, M., Vignola, R., Williams, C. D., Bagatin, R., Latini, A., & Papini, M. P. (2015). Adsorption of hydrocarbons from industrial wastewater onto a silica mesoporous material: Structural and thermal study. *Microporous and mesoporous materials*, *203*, 139–150. https://doi.org/10.1016/j.micromeso.2014.10.021

[13] Bezerra, M. A., Santelli, R. E., Oliveira, E. P., Villar, L. S., & Escaleira, L. A. (2008). Response surface methodology (RSM) as a tool for optimization in analytical chemistry. *Talanta*, *76*(5), 965–977. https://doi.org/10.1016/j.talanta.2008.05.019

[14] Box, G. E. P., & Wilson, K. B. (1992). On the experimental attainment of optimum conditions. In *Breakthroughs in statistics: methodology and distribution* (pp. 270–310). Springer. https://doi.org/10.1007/978-1-4612-4380-9_23%0A%0A

[15] Myers, R. H., Montgomery, D. C., & Anderson-Cook, C. M. (2016). *Response surface methodology: Process and product optimization using designed experiments*. John Wiley & Sons. https://B2n.ir/mx7851

[16] Derringer, G., & Suich, R. (1980). Simultaneous optimization of several response variables. *Journal of quality technology*, *12*(4), 214–219. https://doi.org/10.1080/00224065.1980.11980968

[17] Montgomery, D. C. (2017). *Design and analysis of experiments*. John wiley & sons. https://www.researchgate.net/publication/362079778

[18] Lagergren, S. (1898). About the theory of so-called adsorption of soluble substances. *Kungliga svenska vetenskapsakademiens handlingar*, *24*(4), 1-39. https://www.sid.ir/paper/563615/en

[19] Ho, Y. S., & McKay, G. (1999). Pseudo-second order model for sorption processes. *Process biochemistry*, *34*(5), 451–465. https://doi.org/10.1016/S0032-9592(98)00112-5

[20] Weber Jr, W. J., & Morris, J. C. (1963). Kinetics of adsorption on carbon from solution. *Journal of the sanitary engineering division*, *89*(2), 31–59. https://doi.org/10.1061/JSEDAI.0000430

[21] Langmuir, I. (1918). The adsorption of gases on plane surfaces of glass, mica and platinum. *Journal of the american chemical society*, *40*(9), 1361–1403. https://doi.org/10.1021/ja02242a004

[22] Freundlich, H. (1907). Über die adsorption in lösungen. *Zeitschrift für physikalische chemie*, *57*(1), 385–470. https://www.degruyterbrill.com/document/doi/10.1515/zpch-1907-5723/html

[23] American Public Health Association. (1926). *Standard methods for the examination of water and wastewater* (Vol. 6). American public health association. https://books.google.com/books/about/Standard_Methods_for_the_Examination_of.html?id=V2LhtAEACAAJ

[24] Lei, C., Hu, Y., & He, M. (2013). Adsorption characteristics of triclosan from aqueous solution onto cetylpyridinium bromide (CPB) modified zeolites. *Chemical engineering journal*, *219*, 361–370. https://doi.org/10.1016/j.cej.2012.12.099.

[25] Al-Ghouti, M. A., Al-Kaabi, M. A., Ashfaq, M. Y., & Da'na, D. A. (2019). Produced water characteristics, treatment and reuse: A review. *Journal of water process engineering*, *28*, 222–239. https://doi.org/10.1016/j.jwpe.2019.02.001

[26] Suchithra, P. S., Vazhayal, L., Mohamed, A. P., & Ananthakumar, S. (2012). Mesoporous organic-inorganic hybrid aerogels through ultrasonic assisted sol-gel intercalation of silica-PEG in bentonite for effective removal of dyes, volatile organic pollutants and petroleum products from aqueous solution. *Chemical engineering journal*, *200*, 589–600. https://doi.org/10.1016/j.cej.2012.06.083

[27] Yu, Y., Shapter, J. G., Popelka-Filcoff, R., Bennett, J. W., & Ellis, A. V. (2014). Copper removal using bio-inspired polydopamine coated natural zeolites. *Journal of hazardous materials*, *273*, 174–182. https://doi.org/10.1016/j.jhazmat.2014.03.048

[28] Al-Sareji, O. J. O. (2020). Removal of COD and TOC from domestic wastewater by using alum and peels of sunflowers seeds as natural coagulant. *EurAsian journal of biosciences*, *14*, 2011–2014. https://www.researchgate.net/publication/343127733

[29] Dąbrowski, A. (2001). Adsorption—from theory to practice. *Advances in colloid and interface science*, *93*(1–3), 135–224. https://doi.org/10.1016/S0001-8686(00)00082-8

[30] Shi, S., Qu, Y., Ma, F., & Zhou, J. (2014). Bioremediation of coking wastewater containing carbazole, dibenzofuran, dibenzothiophene and naphthalene by a naphthalene-cultivated Arthrobacter sp. W1. *Bioresource technology*, *164*, 28–33. https://doi.org/10.1016/j.biortech.2014.04.010

[31] Foo, K. Y., & Hameed, B. H. (2010). Insights into the modeling of adsorption isotherm systems. *Chemical engineering journal*, *156*(1), 2–10. https://doi.org/10.1016/j.cej.2009.09.013

[32] Gupta, V. K., Carrott, P. J. M., Ribeiro Carrott, M. M. L., & Suhas. (2009). Low-cost adsorbents: Growing approach to wastewater treatment—A review. *Critical reviews in environmental science and technology*, *39*(10), 783–842. https://doi.org/10.1080/10643380801977610

[33] Ali, I., Asim, M., & Khan, T. A. (2012). Low cost adsorbents for the removal of organic pollutants from wastewater. *Journal of environmental management*, *113*, 170–183. https://doi.org/10.1016/j.jenvman.2012.08.028

[34] Sorokhaibam, L. G., & Ahmaruzzaman, M. (2014). *Phenolic wastewater treatment: Development and applications of new adsorbent materials*. In *Industrial wastewater treatment, recycling and reuse* (pp. 323-368). Elsevier. https://www.researchgate.net/publication/288171342

[35] Vjunov, A., Fulton, J. L., Huthwelker, T., Pin, S., Mei, D., Schenter, G. K., … ., & Lercher, J. A. (2014). Quantitatively probing the Al distribution in zeolites. *Journal of the american chemical society*, *136*(23), 8296–8306. https://doi.org/10.1021/ja501361v

[36] Ho, Y. S. (2006). Review of second-order models for adsorption systems. *Journal of hazardous materials*, *136*(3), 681–689. https://doi.org/10.1016/j.jhazmat.2005.12.043

[37] Jafarinejad, S. (2016). *Petroleum waste treatment and pollution control*. Butterworth-Heinemann. https://www.researchgate.net/publication/318585979

[38] Valdés, H., Sánchez-Polo, M., Rivera-Utrilla, J., & Zaror, C. A. (2002). Effect of ozone treatment on surface properties of activated carbon. *Langmuir*, *18*(6), 2111–2116. https://doi.org/10.1021/la010920a

[39] Budarin, V. L., Clark, J. H., Tavener, S. J., & Wilson, K. (2004). Chemical reactions of double bonds in activated carbon: Microwave and bromination methods. *Chemical communications*, (23), 2736–2737. https://doi.org/10.1039/B411222A

[40] Guo, C., Chen, Y., Chen, J., Wang, X., Zhang, G., Wang, J., … ., & Zhang, Z. (2014). Combined hydrolysis acidification and bio-contact oxidation system with air-lift tubes and activated carbon bioreactor for oilfield wastewater treatment. *Bioresource technology*, *169*, 630–636. https://doi.org/10.1016/j.biortech.2014.07.018

[41] Wang, S., & Peng, Y. (2010). Natural zeolites as effective adsorbents in water and wastewater treatment. *Chemical engineering journal*, *156*(1), 11–24. https://doi.org/10.1016/j.cej.2009.10.029

[42] Yavuz, C. T., Mayo, J. T., Suchecki, C., Wang, J., Ellsworth, A. Z., D'Couto, H., ..., & Colvin, V. L. (2010). Pollution magnet: Nano-magnetite for arsenic removal from drinking water. *Environmental geochemistry and health*, *32*(4), 327-334. https://doi.org/10.1007/s10653-010-9293-y%0A%0A